Five Dimensions for Spectral Colour Management

Steven Le Moan[1], **Jana Blahová**[2], **Philipp Urban**[3], **Ole Norberg**[2]
[1]**Gjøvik University College, Norway**
[2]**Voxvil AB, Sweden**
[3]**Fraunhofer Institute for Computer Graphics Research IGD, Germany**

Abstract

We present a novel extended colour space for low-dimensional spectral colour management, coined LabAB. We discuss design goals and perform a comparison of several approaches to fuse the perceptual information engendered by several illuminants. Results indicate that, with only five dimensions, LabAB conveys significantly no less perceptual information on average than state-of-the-art representations such as the interim connection space LabPQR. We also demonstrate that LabAB can be used for spectral vector error diffusion.

Introduction

Our perception of colours and surface appearances is known to be a complex process that depends on a variety of physical factors and psycho-physical attributes. This complexity often translates to high-dimensional data such as spectral images[1], which represent, typically with 31 channels sampling the visible range of wavelengths, the *reflectance* of an object or scene (i.e. a physical attribute). Such representation allows in turn to estimate the scene's *colour* (i.e. a perceptual attribute) under an arbitrary light source.

In this study, we are interested in representing spectral data (sampling the visible range only) with a limited number of dimensions for spectral colour management. This allows in particular the encoding of device transforms in look-up tables and enables a high run-time performance. Look-up tables are especially useful in applications such as printing, where the relationship between reflectances and ink-coverages is highly non-linear due to subsurface-scattering of light within the substrate (and the inks themselfs). Common forward printer models, such as the Yule-Nielsen Spectral Negebauer model [1, 2, 3] or the Clapper-Yule [4, 5] model are analytically not invertible [6]. In addition, if many inks (e.g. CMYKRGB) are used, spectral forward models are not injective (particularly for dark colours, the same reflectances are obtained for different ink combinations [7]) meaning that optimisation must be used employing some sort of constraints (maximise black, etc.) to obtain a desired ink combination. In such cases an analytical function mapping reflectances to ink-area-coverages simply does not exist and a look-up table must be employed. Incidentally, gamut mapping transformations can also be encoded into the same look-up table for faster processing.

[1] Also referred to as *multi-* or *hyper*-spectral images.

Though traditional colour management utilises one illuminant (e.g. CIE D50 in the ICC workflow) as sole reference for perceptual assessment, *spectral* colour management is intended for applications that require a colorimetric accuracy under more than just one viewing configuration such as security printing, catalogue printing or digital archiving for cultural heritage. In such reproduction workflows, spectral reflectance is considered instead of colour and it must be processed in a perceptually-driven and computationally-efficient fashion. This implies two important design goals for the data used in spectral colour management: it must be **perceptually meaningful**, and have a **low dimensionality**. Additionally, spectral colour management should *improve* traditional colour management, and therefore must allow at least the same quality under a reference illuminant (e.g. CIE D50). This means that the representation must also contain **three colour channels for daylight**. Finally, the representation must also of course be **representative of the original reflectance data**.

In a recent conference paper [8], we proposed a new Extended Colour Space (ECS) coined LabAB, intended to be used in spectral colour management workflows. In this paper, we investigate more thoroughly its design, we provide new evidence of its efficiency and discuss its use for halftoning and colorant separation via spectral vector error diffusion.

Related work and contributions

Early work on developing an efficient representation for spectral colour management include Derhak *et al.*'s **LabPQR** [9, 10]. It contains three colorimetric components (CIE LAB with CIE D50 white point) and three physical ones (PQR) which represent the first three principal components (obtained by Principal Component Analysis - PCA) of the residual error engendered by reconstruction from the three first components, on a training set of reflectances consisting of the printer's spectral gamut. Because it is dependent on a specific device's gamut, and therefore optimised for the communication between a reflectance based profile connection space and said output device, LabPQR is referred to as an *interim connection space*, rather than an ECS. We argue however that LabPQR can be used as an ECS simply by assuming that the aforementioned training set is representative of a large variety of natural reflectances, and not just representative of a device. Wu *et al.*[11] later suggested a **weighted LabPQR** which was shown to provide slightly better colorimetric accuracy. However, one major drawback of LabPQR is that its last three dimensions are not perceptually meaningful, which limits its applicability and, in particular, reduces the meaningfulness of look-up tables linear interpolations [12] since PQR distances are not well correlated to perceived differences. In practice, perceptual uniformity is not crucial if the number of grid points in the table is very high, i.e. interpolation errors are rather small. However if the number of dimensions increase, this comes to the expense of very big tables. A perceptually uniform colour space is beneficial for easily selecting the grid point location (a regular grid can be used) and to meaningfully judge the gradients within the transformation. Additionally, LabPQR relies on a training set of reflectances to generate the PQR channels and is therefore dependent on how representative this set is of a given application. Similar approaches were used in the design of **WSPCA+** [13], and **XYZLMS** [14]. Again, the drawback of these representations is the lack of perceptual meaning of some of their components.

In [15], Nakaya and Ohta suggested two alternative representations: **Lab2**, which consists of the concatenation of two CIE LAB colour spaces with different white points (CIE D65 and CIE A) and **LabRGB**, of which last three dimensions are trigonometric functions roughly representing the spectral distribution of the red, green and blue ranges of wavelengths. While Lab2 can only represent two illuminants, LabRGB has the same disadvantage as LabPQR in that its last three dimensions convey little perceptual information. The idea of concatenating two perceptually meaningful colour spaces was further investigated in [16], where Zhang *et al.*suggested to use a database of illuminants, from which two or three representatives were extracted via PCA. These representatives were then used as white points of concatenated CIE XYZ spaces, which were referred to as **ICS_2SI** and **ICS_3SI** (Interim Connection Space with 2/3 Synthetic Illuminants). However, as we will demonstrate in this study, PCA may not be the optimal strategy to extract a representative illuminant from a set of spectral power distributions.

As far as we know, all existing representations of reflectance data for spectral colour management utilise six dimensions at least. In this paper, we propose one which works with five, coined **LabAB**. We rely on previous work [8, 12] and extend it by suggesting design goals, comparing different methods to extract a representative spectral power distribution of radiance from a set, and presenting results of a successful application of LabAB to spectral vector error diffusion for digital halftoning and colorant separation.

Notations

In the remainder of this paper, we note $\mathbf{r}$ an N-dimensional pixel (vector) representing a reflectance spectrum. We assume that $N > 3$ (typically $N = 31$ resulting from sampling the visible wavelength range from 400700nm in 10 nm steps). In order to represent colour, we use the perceptually uniform and hue-linear LAB2000HL space [17] within which the Euclidean distance approximates the CIE DE2000 colour-difference equation. We note $\mathbf{L}_{00\mathrm{HL}}$, $\mathbf{a}_{00\mathrm{HL}}$ and $\mathbf{b}_{00\mathrm{HL}}$ the components of LAB2000HL and $\mathbf{r}^{\mathbf{i}}_{\mathrm{Lab}}$ the colour (three-dimensional vector) of $\mathbf{r}$ under illuminant $\mathbf{i}$, as observed by the 2° CIE standard observer and represented in LAB2000HL. Note that we consider a model of chromatic adaptation to the CIE D50 illuminant when converting reflectance to colour, in order to account for the ability of our visual system to adjust to various viewing conditions. We used the CAT02 transform [18], with the corrected XYZ-to-RGB conversion matrix proposed in [19], in order to avoid paradoxical (negative) RGB values.

For a given application, we note $\mathbf{\Theta}$ a set of M representative spectral power distributions of illuminants. For instance, if the application is spectral printing for outside viewing, $\mathbf{\Theta}$ should contain a number of different daylight spectra. Matrices $\mathbf{\Omega}$ and $\mathbf{\Omega}'$ contain respectively a training and testing set of reflectances. Accordingly, $\mathbf{r}^{\mathbf{\Theta}}_{\mathrm{Lab}}$ corresponds to the set of M tristimuli generated by $\mathbf{r}$ under all illuminants in $\mathbf{\Theta}$.

Designing a low-dimensional representation of spectral reflectance

In the introduction, we suggested four design goals for an ECS in spectral colour management:

- perceptually uniform (for meaningful look-up table linear interpolations),
- low-dimensional (for fast processing),
- particularly representative of daylight rendering (to compete with colorimetric workflows),
- overall representative of the spectral data.

In order to satisfy the first goal, we propose to use exclusively channels from a colour space with perceptually uniformity. We start with the idea initially presented in [15] to concatenate two colour spaces representing different illuminants. In this section, we discuss which white points should be used for these two colour spaces. Then we demonstrate that redundancy in the lightness channels can be exploited to reduce the dimensionality of the representation to only five.

Representative illuminants

Assuming that $\mathbf{\Theta}$ is representative of the variety of illuminants under which $\mathbf{r}$ should be observed (with respect to a given application), we can consider the following equivalence between *physical* and *perceptual* data:

$$\mathbf{r} \equiv \mathbf{r}^{\mathbf{\Theta}}_{\mathrm{Lab}}, \forall \mathbf{r} \in \mathbf{\Omega} \cup \mathbf{\Omega}'. \quad (1)$$

However, $\mathbf{r}^{\mathbf{\Theta}}_{\mathrm{Lab}}$ has a dimensionality equals to three times the number of illuminants in $\mathbf{\Theta}$. In order to satisfy the second design goal (low dimensionality), we will demonstrate that $\mathbf{r}^{\mathbf{\Theta}}_{\mathrm{Lab}}$ contains a certain amount of redundancy, which can be exploited to a large extent for data reduction. We suggest that $\mathbf{\Theta}$ can be *represented* by two illuminants only (noted $\mathbf{i}_\alpha$ and $\mathbf{i}_\beta$), so that we can consider the following equivalence:

$$\mathbf{r}^{\mathbf{\Theta}}_{\mathrm{Lab}} \equiv \mathbf{r}^{\{\mathbf{i}_\alpha,\mathbf{i}_\beta\}}_{\mathrm{Lab}}, \forall \mathbf{r} \in \mathbf{\Omega} \cup \mathbf{\Omega}'. \tag{2}$$

In order to reach the third design goal (three colour channels for daylight), we set $\mathbf{i}_\alpha$ to be CIE D50 (which is used as reference illuminant in ICC colour management).

As for the last design goal (representativeness), let us first define what it means for $\mathbf{r}^{\{\mathbf{i}_\alpha,\mathbf{i}_\beta\}}_{\mathrm{Lab}}$ to *represent* $\mathbf{r}^{\mathbf{\Theta}}_{\mathrm{Lab}}$. For spectral colour management we argue that the Euclidean distance in $\mathbf{r}^{\{\mathbf{i}_\alpha,\mathbf{i}_\beta\}}_{\mathrm{Lab}}$ must correlate to the largest possible extent to that in $\mathbf{r}^{\mathbf{j}}_{\mathrm{Lab}}$, $\forall \mathbf{j} \in \mathbf{\Theta}$, mainly to ensure that the interpolation in profiles' look-up tables is as meaningful as possible with respect to $\mathbf{\Theta}$, but also to allow perceptually-driven feature extraction (i.e. for spectral image quality assessment [20]) and spectral image processing directly in the ECS. This definition also implies that an image $\mathbf{Im}$ represented in the ECS ($\mathbf{Im}^{\{\mathbf{i}_\alpha,\mathbf{i}_\beta\}}_{\mathrm{Lab}}$) retains most of the perceived *contrast*[2] in $\mathbf{Im}$ with respect to $\mathbf{\Theta}$. Note that the preservation of distance has been used as a dimensionality reduction quality assessment criterion in the remote sensing literature (see e.g. [21]). It translates to finding the solution to the following non-convex optimisation problem:

$$\mathbf{i}_{\mathrm{opt1}} = \arg\max_{\mathbf{i}_\beta} \sum_{\mathbf{j}\in(\mathbf{\Theta}\setminus\mathbf{\Theta}_\alpha)} \rho\left(\mathbf{\Delta}^{\mathbf{i}_\beta}_{\mathbf{\Omega},\mathrm{Lab}}, \mathbf{\Delta}^{\mathbf{j}}_{\mathbf{\Omega},\mathrm{Lab}}\right), \tag{3}$$

where $\rho(\mathbf{x},\mathbf{y})$ is the linear correlation coefficient between $\mathbf{x}$ and $\mathbf{y}$, $\mathbf{\Theta}_\alpha$ is the set of spectral power distributions which are already well represented by $\mathbf{i}_\alpha$ (in this study, we consider that $\mathbf{\Theta}_\alpha = \mathbf{i}_\alpha$) and $\mathbf{\Delta}^{\mathbf{i}}_{\mathbf{\Omega},\mathrm{Lab}}$ is the vector of perceptual distances between all pairs of tristimuli from reflectances in the training set $\mathbf{\Omega}$, observed under illuminant $\mathbf{i}$. The optimal solution $\mathbf{i}_{\mathrm{opt1}}$ can be estimated for example by a quasi-Newton method such as the Broyden-Fletcher-Goldfarb-Shanno algorithm (see [22]).

Additionally, we would like to suggest a second way to define said *representativeness*, which would be more in line with an application such as perceptually lossless compression. It is as follows: $\mathbf{r}^{\{\mathbf{i}_\alpha,\mathbf{i}_\beta\}}_{\mathrm{Lab}}$ represents $\mathbf{r}^{\mathbf{\Theta}}_{\mathrm{Lab}}$ if it permits to generate a reconstruction $\hat{\mathbf{r}} \approx \mathbf{r}$, so that all tristimuli in $\hat{\mathbf{r}}^{\mathbf{\Theta}}_{\mathrm{Lab}}$ and $\mathbf{r}^{\mathbf{\Theta}}_{\mathrm{Lab}}$ are identical, up to an estimated Just-Noticeable-Difference (JND) of $\Delta E_{00\mathrm{HL}} = 1$.

The reconstruction method we used in this study relies on the estimation of a transformation matrix from ECS to reflectance, as in [8]. First, the training set of reflectances $\mathbf{\Omega}$ is transformed linearly to an XYZXYZ space with $\mathbf{i}_\alpha$ and $\mathbf{i}_\beta$ as white points and the result is noted $\mathbf{\Omega}^{\{\mathbf{i}_\alpha,\mathbf{i}_\beta\}}_{\mathrm{XYZXYZ}}$. The transformation matrix from XYZXYZ back to reflectance is then estimated using the pseudoinverse method:

$$\mathbf{T}(\mathbf{i}_\alpha,\mathbf{i}_\beta) = \left[\mathbf{\Omega}^{\{\mathbf{i}_\alpha,\mathbf{i}_\beta\}}_{\mathrm{XYZXYZ}}\right]^{+}\mathbf{\Omega} \tag{4}$$

[2] Here we assume a general definition of contrast.

and applied to the ECS representation of the testing set $\mathbf{\Omega}'^{\{\mathbf{i}_\alpha,\mathbf{i}_\beta\}}_{\mathrm{XYZXYZ}}$ so that:

$$\mathbf{\Omega}'^{\{\mathbf{i}_\alpha,\mathbf{i}_\beta\}}_{\mathrm{XYZXYZ}}\mathbf{T}(\mathbf{i}_\alpha,\mathbf{i}_\beta) = \hat{\mathbf{\Omega}}'(\mathbf{i}_\alpha,\mathbf{i}_\beta) \approx \mathbf{\Omega}' \tag{5}$$

This second definition of *representativeness* implies that the ECS encodes most of the perceptual information in $\mathbf{r}^{\mathbf{\Theta}}_{\mathrm{Lab}}$. It is best satisfied by the solution to the following optimisation problem:

$$\mathbf{i}_{\mathrm{opt2}} = \arg\min_{\mathbf{i}_\beta} \left\| \mathbf{\Omega}'^{\mathbf{\Theta}}_{\mathrm{Lab}} - \hat{\mathbf{\Omega}}'^{\mathbf{\Theta}}_{\mathrm{Lab}}(\mathbf{i}_\alpha,\mathbf{i}_\beta) \right\|_F, \tag{6}$$

where $\mathbf{\Omega}'^{\mathbf{\Theta}}_{\mathrm{Lab}}$ is a matrix containing the set of all tristimuli obtained from all reflectances in $\mathbf{\Omega}'$ under all illuminants in $\mathbf{\Theta}$, and $\hat{\mathbf{\Omega}}'^{\mathbf{\Theta}}_{\mathrm{Lab}}(\mathbf{i})$ is the equivalent matrix obtained from the reconstructed set $\hat{\mathbf{\Omega}}'(\mathbf{i})$. Also, $\|.\|_F$ represents the Frobenius norm. Note that $\mathbf{i}_{\mathrm{opt2}}$, unlike $\mathbf{i}_{\mathrm{opt1}}$, is dependent on $\mathbf{i}_\alpha$ and on the testing set $\hat{\mathbf{\Omega}}'$. Here too, the optimal solution can be estimated by a quasi-Newton method.

We suggest to leave the two aforementioned optimisation problems unconstrained, which implies that $\mathbf{i}_{\mathrm{opt1}}$ and $\mathbf{i}_{\mathrm{opt2}}$ can potentially have any shape (i.e. not necessarily smooth) and range (i.e. not necessarily positive), and therefore may not be physically plausible. However, both these problems pertain to maximising a resemblance to perceptual data, which can be interpreted as maximising perceptual meaningfulness. Therefore, even if $\mathbf{i}_{\mathrm{opt1}}$ or $\mathbf{i}_{\mathrm{opt2}}$ are not plausible or measurable in a physical sense, we argue that the resulting colour tristimuli in $\mathbf{\Omega}^{\mathbf{i}_{\mathrm{opt1}}}_{\mathrm{Lab}}$ and $\mathbf{\Omega}^{\mathbf{i}_{\mathrm{opt2}}}_{\mathrm{Lab}}$ are (almost) perceptually meaningful. In our experiments (described in the next section), we observed that both sets contained only valid colorimetric values.

These two optimal illuminants are dependent on the training set $\mathbf{\Omega}$ and their suitability for use with $\mathbf{\Omega}'$ is therefore dependent on how representative the former is of the latter. Alternatively, we suggest the following solutions, which rely only on $\mathbf{\Theta}$ to compute $\mathbf{i}_\beta$:

- First principal component of $\mathbf{\Theta}$ (as in [16]): $\mathbf{i}_{\mathrm{PCA}}$.
- First principal component of $\mathbf{\Theta}$, when the latter is weighted by a combination of the CIE XYZ 2° standard observer functions, as suggested in [23, 11]: $\mathbf{i}_{\mathrm{wPCA}}$. We used the following weighting function:

$$w = \frac{\sqrt{\bar{x}(\lambda) + \bar{y}(\lambda) + \bar{z}(\lambda)}}{1.46503}, \tag{7}$$

  as suggested in [11].
- First principal component of $\mathbf{\Theta}$, after maximal decorrelation from $\mathbf{i}_\alpha$ by orthogonal subspace projection (as in [8]): $\mathbf{i}_{\mathrm{dPCA}}$.
- Average spectrum: $\mathbf{i}_{\mathrm{av}}$.
- Median spectrum: $\mathbf{i}_{\mathrm{med}}$.

Note that $\mathbf{i}_{\mathrm{PCA}}$ and $\mathbf{i}_{\mathrm{wPCA}}$ were scaled between the minimal and maximal values in the set that they represent.

Table 1: Linear correlation coefficients of pairwise perceptual distances CPD($\mathbf{i}$) (means, standard deviations and minimum values). The worst results are shown in bold font.

		$\mathbf{i}_{\text{PCA}}$	$\mathbf{i}_{\text{wPCA}}$	$\mathbf{i}_{\text{dPCA}}$	$\mathbf{i}_{\text{av}}$	$\mathbf{i}_{\text{med}}$	$\mathbf{i}_{\text{opt1}}$	$\mathbf{i}_{\text{opt2}}$
$\mathbf{\Theta}_{\text{All}}$	mean	**0.772**	0.983	**0.779**	0.983	0.982	0.983	**0.850**
	σ^2	0.090	0.014	0.089	0.014	0.019	0.016	0.058
	min	**0.649**	0.934	**0.658**	0.932	0.918	0.928	**0.764**

Comparison

We compared all the suggested representative illuminants in terms of preservation of distances and reconstruction error. We used the 1269 Munsell matte colour chips (421 dimensions representing the range 380nm - 800nm) as reference reflectance data for $\mathbf{\Omega}$, as well as the representative Standard Object Colour Spectra (SOCS) database [24] as testing data ($\mathbf{\Omega'}$). We used a collection of 40 illuminants' spectral power distributions noted $\mathbf{\Theta}_{\text{All}}$, made of four equally-sized subgroups: 10 daylights ($\mathbf{\Theta}_{\text{Day}}$), 10 tungsten lights ($\mathbf{\Theta}_{\text{Tun}}$), 10 fluorescent lights ($\mathbf{\Theta}_{\text{Fluo}}$) and 10 LED lights ($\mathbf{\Theta}_{\text{LED}}$). These illuminants were selected randomly from the National Gallery's set [25] as well as from the University of Eastern Finland's daylights set [26] and the CIE standard illuminants. They were all normalised to have a maximal value of 1. Figure 1 shows each subset and its representative illuminants.

For comparison, we used two criteria: the Correlations of Perceptual Distances (CPD) in $\mathbf{\Omega'}$, computed as follows:

$$\text{CPD}(\mathbf{i}) = \left\{\rho\left(\mathbf{\Delta}^{\mathbf{i}}_{\mathbf{\Omega'},\text{Lab}}, \mathbf{\Delta}^{\mathbf{j}}_{\mathbf{\Omega'},\text{Lab}}\right) \mid \mathbf{j} \in \mathbf{\Theta}\right\}, \tag{8}$$

where $\rho\left(\mathbf{x},\mathbf{y}\right)$ represents the linear correlation coefficient between $\mathbf{x}$ and $\mathbf{y}$. As well, we used the reconstruction errors:

$$\epsilon(\mathbf{i}) = \left\{\Delta E_{00HL}\left(\mathbf{\Omega'}^{\mathbf{j}}_{\text{Lab}}, \hat{\mathbf{\Omega}}'^{\mathbf{j}}_{\text{Lab}}\left(\mathbf{i}_\alpha, \mathbf{i}\right)\right) \mid \mathbf{j} \in \mathbf{\Theta}\right\}. \tag{9}$$

Table 1 shows the statistics of CPD while Table 2 shows that of the reconstruction errors. Note that the correlations obtained for each subset of $\mathbf{\Theta}_{\text{All}}$ were all above 0.95 and not significantly different from another. We report only the results for the whole set.

These results suggest that:

- The two criteria for representativeness (preservation of distances and minimal reconstruction error) are not compatible as $\mathbf{i}_{\text{opt1}}$ gives poor results in terms of the second criterion, while $\mathbf{i}_{\text{opt2}}$ gives poor results in terms of the first.
- One illuminant can be enough to carry the pairwise relations (i.e. contrast) between reflectances in $\mathbf{\Omega'}$ with a fairly high linear correlation (≥ 0.93).
- With only two illuminants, one can convey valuable information which allow, through reflectance reconstruction, to estimate the perceived difference under a variety of illuminants with a high accuracy: $\mathbf{i}_{\text{opt2}}$ engenders an average reconstruction error that is significantly smaller[3] than $\Delta E_{\text{00HL}} = 1$, which we assume represents a just noticeable difference.
- Regular PCA should not be the preferred strategy to extract a representative illuminant, even when $\mathbf{\Theta}$ is de-correlated from $\mathbf{i}_\alpha$. $\mathbf{i}_{\text{PCA}}$ and $\mathbf{i}_{\text{dPCA}}$ perform significantly worse than other illuminants in terms of preservation of distances. Instead, $\mathbf{i}_{\text{av}}$ seems to offer a better compromise between the two *representativeness* criteria: it performs significantly better or similarly to all others in terms of preservation of pairwise distances and yields smaller reconstruction errors than $\mathbf{i}_{\text{med}}$ and $\mathbf{i}_{\text{opt1}}$ on $\mathbf{\Theta}_{\text{All}}$. Although $\mathbf{i}_{\text{wPCA}}$ seems to yield similar performances to $\mathbf{i}_{\text{av}}$, we decided to pursue this study using the latter, because of its remarkable simplicity. Therefore $\mathbf{i}_\beta = \mathbf{i}_{\text{av}}$ in the remainder of this paper.

Redundancies in perceptual attributes across viewing conditions

In order to identify redundancies in $\mathbf{r}^{\{\mathbf{i}_\alpha,\mathbf{i}_\beta\}}_{\text{Lab}}$, we analysed the behavior of several perceptual features across viewing conditions (illuminants). We used the components of the perceptually uniform LAB2000HL colour space, but, in order to also have an insight into how chroma and hue behave across illuminants, we computed these components as follows:

$$\mathbf{C}_{\text{00HL}} = \sqrt{\mathbf{a}^2_{\text{00HL}} + \mathbf{b}^2_{\text{00HL}}} \tag{10}$$

$$\mathbf{H}_{\text{00HL}} = \arctan\left(\frac{\mathbf{b}_{\text{00HL}}}{\mathbf{a}_{\text{00HL}}}\right) \tag{11}$$

where $\mathbf{C}_{\text{00HL}}$ and $\mathbf{H}_{\text{00HL}}$ are respectively the chroma and hue components.

We then studied the variability of these five features ($\mathbf{L}_{\text{00HL}}$, $\mathbf{a}_{\text{00HL}}$, $\mathbf{b}_{\text{00HL}}$, $\mathbf{C}_{\text{00HL}}$ and $\mathbf{H}_{\text{00HL}}$) in $\mathbf{\Omega}$. We used Shannon's entropy [27] as a measure of variability and computed that, in $\mathbf{\Theta}_{\text{All}}$, of each feature (with chromatic adaptation). Table 3 shows the mean values, standard deviations and maxima obtained in $\mathbf{\Omega}$.

These results suggest that the entropy of lightness, as represented in LAB2000HL, is significantly smaller than that of any of the selected chromatic attributes. This is in accordance with the conclusions in [28], were we used

[3] Two mean values m_1 and m_2 with corresponding standard deviations σ_1 and σ_2 are significantly different if $m_1 + \sigma_1 < m_2 - \sigma_2$ (if $m_1 < m_2$) or $m_2 + \sigma_2 < m_1 - \sigma_1$ (if $m_1 > m_2$).

Table 2: Statistics of reconstruction errors $\epsilon(\mathbf{i})$ (means, standard deviations and maximum values). The best results are shown in bold font.

		$\mathbf{i}_{\text{PCA}}$	$\mathbf{i}_{\text{wPCA}}$	$\mathbf{i}_{\text{dPCA}}$	$\mathbf{i}_{\text{av}}$	$\mathbf{i}_{\text{med}}$	$\mathbf{i}_{\text{opt1}}$	$\mathbf{i}_{\text{opt2}}$
$\mathbf{\Theta}_{\text{All}}$	mean	0.01	0.02	0.46	0.75	1.81	1.64	**0.29**
	σ^2	0.61	0.68	0.59	0.71	1.35	1.19	0.39
	max	11.36	9.28	12.21	10.49	12.67	13.39	**8.89**
$\mathbf{\Theta}_{\text{Day}}$	mean	0.11	0.16	0.58	0.13	0.13	0.12	**0.09**
	σ^2	0.26	0.30	0.65	0.28	0.27	0.27	0.24
	max	5.21	6.67	7.43	5.64	6.25	5.13	**4.17**
$\mathbf{\Theta}_{\text{Tun}}$	mean	0.10	0.11	0.24	0.11	0.10	0.13	**0.08**
	σ^2	0.19	0.23	0.38	0.18	0.18	0.18	0.19
	max	4.23	4.60	8.64	4.25	4.21	3.96	**3.89**
$\mathbf{\Theta}_{\text{Fluo}}$	mean	0.66	0.70	0.67	0.69	0.65	0.79	0.38
	σ^2	0.82	1.04	0.84	0.97	0.92	1.00	0.39
	max	11.24	20.55	11.00	18.53	14.78	21.91	**8.86**
$\mathbf{\Theta}_{\text{LED}}$	mean	1.73	1.99	0.77	1.69	1.07	1.64	0.45
	σ^2	1.25	1.34	0.84	1.24	0.97	1.23	0.56
	max	14.77	13.85	17.03	14.86	13.62	15.14	**10.28**

instead image-difference features to demonstrate that, in order to compare two spectral images, lightness can be considered as redundant across illuminants. Here we show, on a representative set of spectra, and considering only pixel attributes (as opposed to *image-difference* attributes) that this redundancy seems to be significant in comparison to that of $\mathbf{a}_{00\text{HL}}$ and $\mathbf{b}_{00\text{HL}}$ for several sets of illuminants. We also suggest that $\mathbf{L}_{00\text{HL}}$ is significantly more redundant than $\mathbf{C}_{00\text{HL}}$ only in the case of $\mathbf{\Theta}_{\text{All}}$ and than $\mathbf{H}_{00\text{HL}}$ except for $\mathbf{\Theta}_{\text{Day}}$ and $\mathbf{\Theta}_{\text{Tun}}$. Finally, we observe from these results that the redundancy in lightness seems more dependent on $\mathbf{r}$ than that of other attributes in all illuminants sets because it yields large standard deviations in $\mathbf{\Omega}$.

Table 3: Mean values and standard deviations of the estimated entropy of several perceptual attributes (with chromatic adaptation). Values are given in *bits*. The entropy measures the number of bits required to encode the full range of the corresponding data. According to these results, lightness is significantly more predictable than any chromatic attributes.

		$\mathbf{L}_{00\text{HL}}$	$\mathbf{a}_{00\text{HL}}$	$\mathbf{b}_{00\text{HL}}$	$\mathbf{C}_{00\text{HL}}$	$\mathbf{H}_{00\text{HL}}$
$\mathbf{\Theta}_{\text{All}}$	mean	**3.75**	4.97	4.91	4.79	4.63
	σ^2	0.66	0.24	0.17	0.27	0.22

In view of these observations, we propose to further reduce the dimensionality of $\mathbf{r}_{\text{Lab}}^{\{\mathbf{i}_\alpha,\mathbf{i}_\beta\}}$ by considering the approximation $\mathbf{L}_{00\text{HL}}^{\mathbf{i}_\alpha} \approx \mathbf{L}_{00\text{HL}}^{\mathbf{i}_\beta}$. We computed the linear correlation coefficients between $\mathbf{L}_{00\text{HL}}^{\mathbf{i}_\alpha}$ and $\mathbf{L}_{00\text{HL}}^{\mathbf{i}_\beta}$ for each subset of illuminants and observed no coefficient below 0.97, which indicates that all candidate illuminants are suitable to make the aforementioned approximation valid. Incidentally, the corresponding coefficients for the Chroma and Hue channels are of course lower, particularly for $\mathbf{i}_{\text{PCA}}$ and $\mathbf{i}_{\text{opt2}}$.

LabAB

Based on the conclusions of the previous sections and in view of the design goals mentionned in the introduction, we propose a perception-aware, five-dimensional ECS coined LabAB, which consists of the concatenation of LAB2000HL components for $\mathbf{i}_\alpha = $ CIE D50 and the chromatic components of LAB2000HL for $\mathbf{i}_\beta = \mathbf{i}_{\text{av}}$:

$$\mathbf{r} \equiv \left\{\mathbf{r}_{\text{Lab}}^{\mathbf{i}_\alpha}, \mathbf{r}_{\text{ab}}^{\mathbf{i}_\beta}\right\} \tag{12}$$

Note that both LAB2000HL spaces have the same white point as we use chromatic adaptation.

Comparison with the state-of-the-art

We compared the proposed representation, **LabAB**, with **Lab2** (with $\mathbf{i}_{\text{av}}$ as second illuminant), **Lab2** (with CIE A as second illuminant, as in [15]), **LabPQR** [9], **LabPQ** (same as the latter but without the last component) and **LabRGB** [15]. We used CIE D50 as reference illuminant for the three first colorimetric components of each representation. Those needing training were trained on $\mathbf{\Omega}$ and all were tested on $\mathbf{\Omega}'$. Results are given in $\Delta E_{00\text{HL}}$ units and shown in Table 4.

These results suggest that:

- Using $\mathbf{i}_{\text{av}}$ in Lab2 results in the best reconstruction errors, which are not significantly larger than a JND of $\Delta E_{00\text{HL}} = 1$ for all sets.
- In terms of mean value, using only five dimensions leads to a colorimetric accuracy that is not significantly different from when using a sixth dimension. In terms of maximal error however, it leads to about half the accuracy of **LabAB** ($\mathbf{i}_{\text{av}}$). Intuitively, the reflectances that engender the maximal errors are those that also produce the largest variations of lightness values across $\mathbf{\Theta}$, thus invalidating our assumption

Table 4: Comparison with state-of-the-art in terms of reconstruction error with Ω as training set and Ω' as testing set.

		LabAB (i_{av})	**Lab2** (i_{av})	**Lab2** (CIE A)	**LabPQR**	**LabPQ**	**LabRGB**
$\mathbf{\Theta}_{All}$	mean	0.86	**0.25**	1.56	0.38	0.43	7.56
	σ^2	1.07	0.31	1.34	0.52	0.59	4.68
	max	13.94	**6.98**	14.07	9.93	11.47	31.60
$\mathbf{\Theta}_{Day}$	mean	0.49	**0.03**	1.28	0.18	0.20	7.34
	σ^2	0.63	0.11	1.19	0.22	0.26	4.81
	max	10.81	**3.27**	11.46	4.77	5.58	31.60
$\mathbf{\Theta}_{Tun}$	mean	0.73	**0.07**	1.65	0.27	0.29	7.33
	σ^2	0.92	0.15	1.26	0.44	0.46	4.32
	max	10.01	**3.07**	9.15	8.93	9.53	27.18
$\mathbf{\Theta}_{Fluo}$	mean	0.98	**0.28**	1.43	0.55	0.61	7.78
	σ^2	1.05	0.38	1.45	0.68	0.79	4.88
	max	14.00	**8.62**	12.39	9.93	11.47	28.54
$\mathbf{\Theta}_{LED}$	mean	0.93	**0.28**	1.88	0.52	0.63	7.82
	σ^2	0.94	0.31	1.36	0.52	0.60	4.65
	max	13.60	**7.11**	14.07	8.85	9.16	29.88

that lightness is a redundant feature. In our experiments, we observed that these reflectances seem to have in common that their energy is concentrated over a relatively small range of wavelengths (narrowband), thus making their perceived lightness particularly dependent on the shape of the illuminant's spectral power distribution. Incidentally, these spectra also result in particularly high chroma values. The 20 largest errors were indeed obtained with spectra yielding a chroma greater than 45 $\mathbf{C}_{00HL}$ units under CIED65.

- LabPQ also renders an average accuracy that is not significantly different from that of its six-dimensional counterpart. However, as mentioned in the introduction, the main disadvantage of the PQR components is their lack of perceptual meaning.

Consequently, 5-dimensional LabAB seems to be a reliable alternative to Lab2 or LabPQR for the reproduction of natural reflectances, particularly for those whose lightness varies little in the set of selected illuminants $\mathbf{\Theta}$. LabAB is perceptually meaningful, low dimensional, contains three channels for daylight and is - on average - as representative of the original reflectance data as its 6-dimensional counterparts. Note also that look-up tables for colour management profiles typically use 33 grid points per dimension, which means that tables based on LabAB contain 33 times less entries than that based on e.g. LabPQR, which enables a substantially higher run-time performance.

Application to spectral vector error diffusion

In this section, we provide evidence of the suitability of LabAB for haltoning and colorant separation by spectral vector error diffusion (sVED). First, we give some background information, then we present the experimental setup and the results.

Background information

Digital halftoning is a transformation of continuous-tone images (e.g. 8 bits per pixel) into images with a limited number of colours (e.g. 1 bit per pixel), which can then be reproduced by a printer. Three types of halftoning methods may be considered [29]. First, point processes such as screening or dithering are based on a pixel-by-pixel comparison with a spatially varying threshold. Second, neighborhood processes such as error diffusion require processing of pixels from a local neighborhood. Third, iterative processes such as direct binary search look for the best possible configuration of the binary values in the halftone image requiring several passes through the continuous-tone image.

In this paper, we are interested in the second category of methods and particularly in spectral vector error diffusion, which has the advantage to allow to perform halftoning and colorant separation in one step, and with a smaller computational cost than that of iterative processes.

Error diffusion consists of shaping the quantization noise (resulting from the mapping of a pixel to the printer's gamut) into the image's high frequencies, so as to make it as little perceivable as possible. It consists of two steps: thresholding and diffusion. Thresholding corresponds to mapping a target pixel to a printable (i.e. in-gamut) tristimulus and diffusion consists of propagating the resulting error to neighboring pixels, based on a given error filter such as the well-known Floyd and Steinberg filter [30]. While scalar error diffusion is used to process grayscale images or colour channels independently, vector error diffusion was reported to perform better at preserving the perceived image quality in the halftoning process [31]. Gerhardt *et al.*[32] proposed an extension of colour vector error diffusion for spectral colour reproduction workflows. While originally, reflectance RMSE is used for thresholding and diffusion is made in the reflectance space, it was shown [33] that using a perceptual metric such as ΔE_{94} yields a significantly higher colorimetric accuracy. In this study, we demonstrate that LabAB can be used for perceptually-aware thresholding and error diffusion in sVED.

Experimental setup and results

The printing system utilised to test our model is a Canon imagePrograf iPF5100. This inkjet printer has a 12-colour LUCIA pigment ink set from which we used 10 inks (cyan, magenta, yellow, black, red, green, blue, light cyan, light magenta and gray). For the substrate we used the Canon Matte Photo Paper, 170g/m^2. As input data, ten halftoned 1-bit images (1≡'ink', 0≡'no ink') were generated (one for each ink) and sent to the printer directly without any colour management. Spectral measurements were made using a Spectrolino from Gretag Macbeth at $45^\circ/0^\circ$ measurement geometry. The sampling step was 10nm in the wavelength range of 400700nm.

Note that we used a resolution of 1200 dots-per-inch and a novel multilevel halftoning model [34], which implies that each input pixel corresponds to four output pixels, in order to maximise the size of the printer's gamut. For $\mathbf{\Theta}$, we used only CIE A. For the diffusion filter weights, we tried both Floyd-Steinberg's and Kolpatzik-Bouman's [35] coefficients. The latter consists of two sets: achromatic and chromatic. However, we observed no significant difference between the two. We report only the results obtained with the Floyd-Steinberg coefficients.

For comparison, we measured the colorimetric errors for a set of 600 uniform patches under CIE D50 (reference illuminant) and CIE A and for three different approaches to sVED:

- Approach 1: $\Delta E_{\mathrm{LabAB}} = \frac{3}{4}\Delta E_{\mathrm{Lab}} + \frac{1}{4}\Delta E_{\mathrm{AB}}$ for thresholding (i.e. a weighted Euclidean distance to favorise the reference illuminant where ΔE_{Lab} represents the distance in the first two components of LabAB and ΔE_{AB} represents the distance in the last two ones) and LabAB for diffusion.
- Approach 2: ΔE_{00HL} (for CIE D50) for thresholding and reflectance space for diffusion (similarly to [33], where the authors used ΔE_{94} instead).
- Approach 3: Reflectance RMSE for thresholding and reflectance space for diffusion (as in [34]). Note that this approach is significantly more computationally expensive than the previous one due to the high dimensionality of the reflectance space.

Table 5 depicts the results obtained. It can be seen that, although the mean errors are not significantly different due to the large standard deviations, Approach 1 yields significantly smaller maximal errors than the state-of-the art (Approaches 2 and 3). That Approach 1 is more suited for illuminant A is not surprising as it is the only approach that is optimised for it. However it also seems more suited for illuminant D50, even though Approach 2 is optimised for it. Additionally, these results suggest that spectral vector error diffusion can be performed in only five dimensions while showing better performances than when using the "raw" reflectance data.

Table 5: Colorimetric errors resulting from spectral vector error diffusion on 600 uniform patches.

		Approach 1	Approach 2	Approach 3
D50	mean	2.28	3.17	3.52
	std	**2.05**	2.84	3.48
	max	**14.35**	20.58	28.67
A	mean	2.40	3.28	3.54
	std	**2.10**	2.95	3.48
	max	**17.74**	22.89	27.97

Conclusions

We presented a novel extended colour space for low-dimensional spectral colour management, coined LabAB. We discussed design goals and performed a comparison of several approaches to represent a set of light sources with a single spectral power distribution. Results indicate that, with only five dimensions, LabAB conveys significantly no less perceptual information on average than state-of-the-art representations such as LabPQR. We also demonstrated that LabAB can be used for spectral vector error diffusion.

References

[1] H. E. J. Neugebauer, "Die theoretischen Grundlagen des Mehrfarbenbuchdrucks," *Zeitschrft fr wissenschaftliche Photographie, Photophysik und Photochemie [reprint in [36], translation in [37]]*, vol. 36, pp. 73–89, 1937.

[2] J. A. C. Yule and W. J. Nielsen, "The penetration of light into paper and its effect on halftone reproduction," in *Tech. Assn. Graphic Arts*, 1951, vol. 4, pp. 65–76.

[3] J.A.S. Viggiano, "The Color of Halftone Tints," in *TAGA Proceedings*, 1985, pp. 647–661.

[4] F.R. Clapper and J.A.C. Yule, "The effect of multiple internal reflections on the densities of half-tone prints on paper," *JOSA*, vol. 43, no. 7, pp. 600–603, 1953.

[5] F.R. Clapper and J.A.C. Yule, "Reproduction of color with halftone images," in *Proc. Seventh Ann. Tech. Meet. TAGA*, 1955, pp. 1–14.

[6] P. Urban and R.-R. Grigat, "Spectral-Based Color Separation using Linear Regression Iteration," *Color Research and Application*, vol. 31, pp. 229–238, 2006.

[7] M. R. Rosen, E. F. Hattenberger, and N. Ohta, "Spectral redundancy in a six-ink ink jet printer," *Journal of Imaging Science and Technology*, vol. 48, pp. 194–202, 2004.

[8] Steven Le Moan and Philipp Urban, "A new connection space for low-dimensional spectral color management," in *Measuring, Modeling, and Reproducing Material Appearance*, Maria V. Ortiz Segovia, Philipp Urban, and Jan P. Allebach, Eds., San Francisco, CA, February 2014, vol. 9018, pp. 9018–12, SPIE.

[9] M.W. Derhak and M.R. Rosen, "Spectral Colorimetry using LabPQR - An Interim Connection Space,"

Journal of Imaging Science and Technology, vol. 50, pp. 53–63, 2006.

[10] Shohei Tsutsumi, Mitchell Rosen, and Roy Berns, "Spectral gamut mapping using labpqr," *Journal of Imaging Science and Technology*, vol. 51, no. 6, pp. 473–485, 2007.

[11] Guangyuan Wu, Zhen Liu, Shengwei Yang, Ming Zhu, and Pan Liu, "Weighted LabPQR interim connection space based on human color vision for spectral color reproduction," *Journal of Spectroscopy*, vol. 2014, 2014.

[12] Steven Le Moan and Philipp Urban, "Spectral printing with a CMYKRGB printer: a closer look," in *22nd Color and Imaging Conference*. November 2014, IS&T.

[13] Ying Wang, Sheping Zhai, and Jianyuan Liu, "Dimensionality reduction of multi-spectral images for color reproduction," *Journal of Software*, vol. 8, no. 5, pp. 1180–1185, 2013.

[14] Xiandou Zhang, Qiang Wang, Yong Wang, and Haozhe Wu, "Xyzlms interim connection space for spectral image compression and reproduction," *Optics letters*, vol. 37, no. 24, pp. 5097–5099, 2012.

[15] Fumio Nakaya and Noboru Ohta, "Spectral encoding/decoding using LabRGB," *Journal of Imaging Science and Technology*, vol. 52, no. 4, pp. 40902–1, 2008.

[16] X. Zhang, Q. Wang, J. Li, P. Yang, and J. Yu, "The interim connection space based on human color vision for spectral color reproduction," *Journal of Optical Society of America A*, vol. 29, no. 6, pp. 1027–1034, 2012.

[17] I. Lissner and P. Urban, "Toward a unified color space for perception-based image processing," *IEEE Transactions on Image Processing*, vol. 21, no. 3, pp. 1153–1168, 2012.

[18] CIE Publication No. 159, "A colour appearance model for colour management systems: CIECAM02," Vienna, 2004, CIE Central Bureau.

[19] Changjun Li, Esther Perales, M Ronnier Luo, and Francisco Martínez-Verdú, "Mathematical approach for predicting non-negative tristimulus values using the CAT02 chromatic adaptation transform," *Color Research & Application*, vol. 37, no. 4, pp. 255–260, 2012.

[20] Steven Le Moan and Philipp Urban, "Image-difference prediction: From color to spectral," *IEEE Transactions on Image Processing*, vol. 23, no. 5, pp. 2058–2068, 2014.

[21] M. Cui, A. Razdan, J. Hu, and P. Wonka, "Interactive hyperspectral image visualization using convex optimization," *IEEE Transactions on Geoscience and Remote Sensing*, vol. 47, no. 6, pp. 1673, 2009.

[22] Adrian S Lewis and Michael L Overton, "Nonsmooth optimization via BFGS," *SIAM J. Optimiz*, 2009.

[23] Hannu Laamanen, Tuija Jetsu, Timo Jaaskelainen, and Jussi Parkkinen, "Weighted compression of spectral color information," *JOSA A*, vol. 25, no. 6, pp. 1383–1388, 2008.

[24] Technical Committee ISO/TC 130, Graphic technology, "ISO/TR 16066: Standard object colour spectra database for colour reproduction evaluation (SOCS)," Tech. Rep., 2003.

[25] "Spectral power distribution curves, the national gallery: `http://research.ng-london.org.uk/scientific/spd/`," Accessed on Oct. 5th, 2015.

[26] "Database - daylight spectra, university of eastern finland: `http://cs.joensuu.fi/~spectral/databases/download/daylight.htm`," Accessed on Oct. 12th, 2015.

[27] C.E. Shannon and W. Weaver, "A mathematical theory of communication," *The Bell System Technical Journal*, vol. 27, pp. 379–423, 1948.

[28] Steven Le Moan and Philipp Urban, "Evaluating the perceived quality of spectral images," in *20th International Conference on Image Processing*. September 2013, IEEE.

[29] Jan P Allebach, "Dbs: retrospective and future directions," in *Photonics West 2001-Electronic Imaging*. International Society for Optics and Photonics, 2000, pp. 358–376.

[30] R.W. Floyd and L. Steinberg, "An adaptive algorithm for spatial grey scale," in *Proceedings of the Society of Information Display*. SID, 1976, pp. 75–77.

[31] Niranjan Damera-Venkata and Brian L Evans, "Design and analysis of vector color error diffusion halftoning systems," *Image Processing, IEEE Transactions on*, vol. 10, no. 10, pp. 1552–1565, 2001.

[32] Jérémie Gerhardt and Jon Y Hardeberg, "Spectral colour reproduction by vector error diffusion," in *Conference on Colour in Graphics, Imaging, and Vision*. Society for Imaging Science and Technology, 2006, number 1, pp. 469–473.

[33] Ole Norberg and Daniel Nyström, "Spectral vector error diffusion-promising road or dead end?," in *Color and Imaging Conference*. Society for Imaging Science and Technology, 2012, number 1, pp. 329–334.

[34] Ole Norberg and Daniel Nyström, "Extending color primary set in spectral vector error diffusion by multilevel halftoning," in *IS&T/SPIE Electronic Imaging*. International Society for Optics and Photonics, 2013, pp. 86520M–86520M.

[35] Bernd W Kolpatzik and Charles A Bouman, "Optimized error diffusion for image display," *Journal of Electronic Imaging*, vol. 1, no. 3, pp. 277–292, 1992.

[36] H. E. J. Neugebauer, "Die theoretischen Grundlagen des Mehrfarbenbuchdrucks," in *Proceedings of SPIE: Neugebauer Memorial Seminar on Color Reproduction*, Tokyo, Japan, 1989, vol. 1184, pp. 194–202.

[37] H. E. J. Neugebauer, "The Theoretical Basis of Multicolor Letterpress Printing (Translated D. Wyble and A. Kraushaar)," *Color Research and Application*, vol. 30, pp. 322–331, 2005.

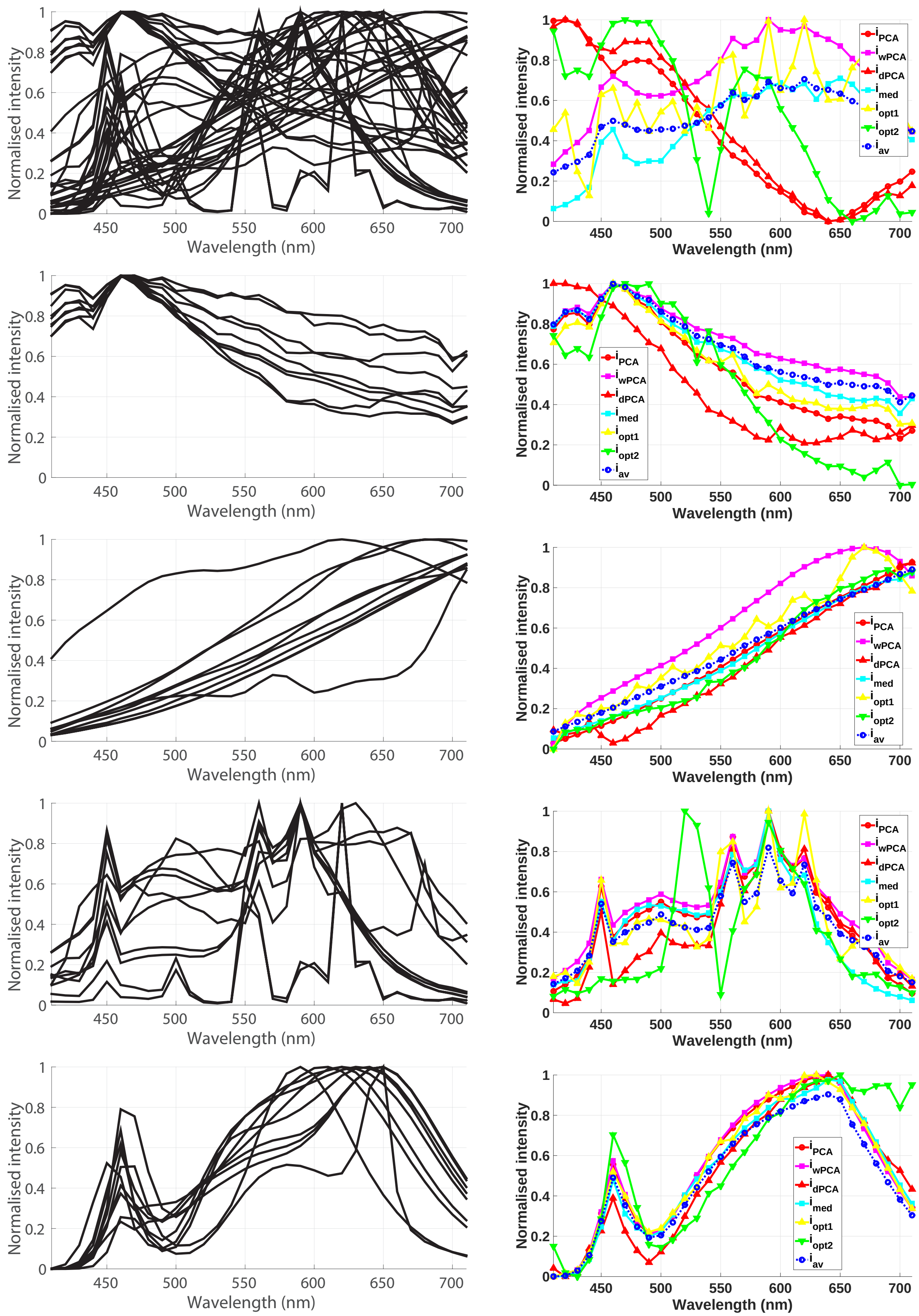

Figure 1. *Illuminants. Left: sets (row-wise: Θ, Θ_{Day}, Θ_{Tun}, Θ_{Fluo}, Θ_{LED}). Right: corresponding representatives. Note that $\mathbf{i}_{opt1}$ and $\mathbf{i}_{opt2}$ were scaled for display.*